Pressure-induced structural changes in liquid cadmium telluride: *Ab initio* molecular dynamics study

Yasuhisa Miyata, Fuyuki Shimojo, and Masaru Aniya
Department of Physics, Kumamoto University, Kumamoto 860-8555, Japan
(Received 18 December 2007; revised manuscript received 27 February 2008; published 28 March 2008)

The structural and electronic properties of liquid CdTe under pressure are studied by *ab initio* molecular dynamics simulations. It is shown that the pressure dependence of the static structure factor observed by the recent x-ray-diffraction experiments is successfully reproduced by our simulations for a wide range of pressure up to about 20 GPa. The population analysis, as well as the electronic density of states, reveals that the covalent-bonding interaction between Cd and Te atoms is retained in the liquid state below 4 GPa. It is found that short-range correlations between like atoms become important at higher pressures accompanying metallization, i.e., Cd-Cd and Te-Te correlations appear in the first-coordination shell around each Cd and Te above about 4 and 8 GPa, respectively.

DOI: 10.1103/PhysRevB.77.125217 PACS number(s): 61.25.Mv, 71.22.+i, 71.15.Pd

I. INTRODUCTION

It is known that the crystalline phases of III-V and II-VI compounds have a tetrahedrally coordinated structure (zinc blende or wurtzite) at ambient pressure.[1] They have partially covalent and partially ionic bonding between atoms. The sequence of pressure-induced structural transformations in crystals depends on such nature of atomic bonding. When crystalline III-V compounds, such as GaSb, InSb, and InAs, are compressed, the tetrahedrally coordinated structure transforms into an intermediate structure (β-tin) before the appearance of the sixfold coordinated structure (rocksalt). On the other hand, crystalline II-VI compounds, such as CdTe and ZnSe, change their structures from the tetrahedrally coordinated structure to the sixfold coordinated structure directly under pressure. This difference in the pressure dependence of the crystal structure is considered to come from the fact that the ionicity of II-VI compounds is larger than that of III-V compounds.

It is natural to expect that a similar sequence of structural changes will occur in the liquid phase under pressure. Using the synchrotron x-ray-diffraction technique, Hattori *et al.* have investigated the pressure dependence of the structural properties of liquid III-V compounds, such as liquid GaSb,[2] liquid InAs,[3] and liquid InSb.[4] They found that, although these liquid compounds show apparently different contraction behaviors from each other, the structural change occurs gradually with increasing pressure. Recently, they have carried out x-ray-diffraction measurements of liquid CdTe, one of the liquid II-VI compounds, under pressure up to about 20 GPa.[5,6] It was found that the structure of liquid CdTe exhibits drastic changes in two pressure regions, 1.8–3.0 and 7.0–9.0 GPa, which means that there exist at least three stable liquid forms. This pressure dependence is different from that in liquid III-V compounds. They explained that the lowest- and intermediate-pressure forms have a similar local structure to the crystalline counterparts, while the highest-pressure form has a different local structure.

Since it is difficult to obtain the partial structures experimentally, computer simulations based on a first-principles theory would be useful to investigate the pressure-induced structural changes in more detail. So far, the structure of liquid CdTe at ambient pressure has been studied by first-principles calculations.[7,8] However, we are unaware of theoretical studies on the pressure dependence. In this paper, we investigate the structural and electronic properties of liquid CdTe under pressure in detail by *ab initio* molecular dynamics (MD) simulations. The purposes of our study are to compare the calculated structure with the experiments and to clarify the detailed mechanism of compression of the liquid under pressure.

II. METHOD OF CALCULATION

The electronic states were calculated using the projector-augmented-wave (PAW) method[9,10] within the framework of the density functional theory (DFT) in which the generalized gradient approximation[11] (GGA) was used for the exchange-correlation energy. The plane-wave cutoff energies are 180 and 1220 eV for the electronic pseudo-wave-functions and the pseudo-charge-density, respectively. The energy functional was minimized using an iterative scheme.[12,13] The Γ point was used for Brillouin zone sampling. As the valence electrons, we included the 4*d*, 5*s*, and 5*p* electrons of Cd and 5*s*, 5*p*, and 5*d* electrons of Te. Other electrons in the lower-energy electronic states of each atom were treated with the frozen-core approximation.

We used a system of 192 (96Cd+96Te) atoms in a cubic supercell under periodic boundary conditions. Using the Nosé–Hoover thermostat technique,[14,15] the equations of motion were solved via an explicit reversible integrator[16] with a time step of $\Delta t = 3.6$ fs. To obtain a liquid state, we began by carrying out an *ab initio* MD simulation for 3.6 ps at a temperature of 2500 K starting from the zinc-blende structure with a number density of 0.0259 Å^{-3}. Since the temperature is relatively high compared with the melting temperature (1400 K) at ambient pressure, the system reached a completely disordered state without the effects of the initial configuration. Then, we decreased the temperature of the system gradually with MD simulations for 7.2 ps at 2000 K, 10.8 ps at 1700 K, and 14.4 ps at 1450 K. The calculated pressure[17,18] was 0.5 GPa at 1450 K, which was estimated

TABLE I. Number densities ρ (Å^{-3}) and temperatures T (K) used in MD simulations. The calculated pressures P (GPa) are also listed.

ρ (Å^{-3})	T (K)	P (GPa)
0.0259	1450	0.5
0.0280	1450	1.2
0.0303	1700	2.4
0.0316	1450	3.1
0.0329	1700	4.6
0.0343	1700	5.9
0.0358	1700	7.6
0.0374	1700	9.7
0.0391	1750	12.3
0.0409	1750	15.5
0.0427	1800	19.5

by taking the time average. Starting from this state, several MD simulations were carried out with different number densities to investigate the pressure dependence. The temperature was set about 50 K above the observed melting temperature[6] at each pressure. The number densities and temperatures used in our simulations as well as the calculated pressures are listed in Table I. The quantities of interest were obtained by averaging over 12.6 ps after the initial equilibration taking at least 1.8 ps. The simulation time for averaging is long enough to achieve good statistics for the static quantities obtained in this study. When we extended MD simulations up to 21.6 ps of total simulation time, changes in the time-averaged quantities were within 5% (typically less than 1%). We may need longer simulations when dynamic quantities, such as the van Hove correlation function, are investigated.

III. RESULTS

A. Structure factors

Figure 1 shows the pressure dependence of the structure factor $S(k)$ of liquid CdTe. The calculated $S(k)$ (solid lines) are compared with the experimental $S(k)$ (open circles) obtained from the recent x-ray-diffraction measurements.[6] We obtained $S(k)$ from partial structure factors $S_{\alpha\beta}(k)$, shown in Figs. 2 and 3, with x-ray form factors. It is seen from Fig. 1 that the calculated results are in good agreement with the experiments in a wide range of pressure. Below 2.4 GPa, there is a plateau between $k=1.9$ and 2.8 Å^{-1} in the profile of $S(k)$. When the pressure is increased, the plateau changes into a peak around $k=2.3$ Å^{-1}. It should be emphasized that the profiles of $S(k)$ above 4.6 GPa are qualitatively different from those below 2.4 GPa, and $S(k)$ at 3.1 GPa has an intermediate profile between them. Moreover, it is found that the profile of $S(k)$ changes between 5.9 and 9.7 GPa, i.e., the first peak shifts to larger k and becomes sharp. Above 9.7 GPa, $S(k)$ has only weak pressure dependence. These observations clearly suggest that liquid CdTe under pressure

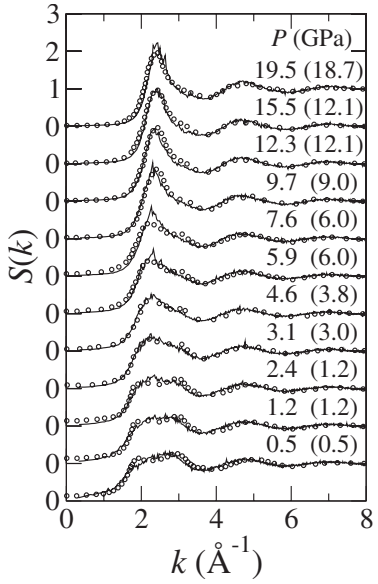

FIG. 1. Pressure dependence of the structure factor $S(k)$ of liquid CdTe. The solid lines and open circles show the calculated and experimental (Ref. 6) results, respectively. The numerals in the parentheses are the pressure observed in the experiments.

is contracted nonuniformly and has some different forms in the liquid state.

The change in the profile of $S(k)$ is well understood from the pressure dependence of the partial $S_{\alpha\beta}(k)$ shown in Figs. 2 and 3. Although $S_{\mathrm{TeTe}}(k)$ has a sharp peak at about $k=1.9$ Å^{-1} below 2.4 GPa, there exists only a shoulder around the same wave number in $S(k)$ because of the cancellation due to the existence of a negative dip in $S_{\mathrm{CdTe}}(k)$. Also, we

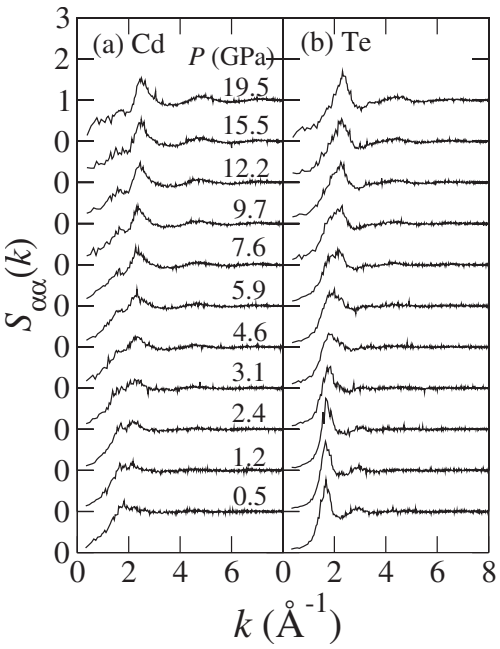

FIG. 2. Pressure dependence of the Ashcroft–Langreth partial structure factors $S_{\alpha\alpha}(k)$ of liquid CdTe for α=(a) Cd and (b) Te.

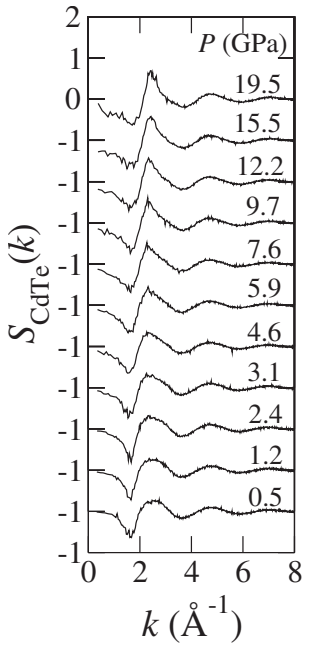

FIG. 3. Pressure dependence of the Ashcroft-Langreth partial structure factor $S_{CdTe}(k)$ of liquid CdTe.

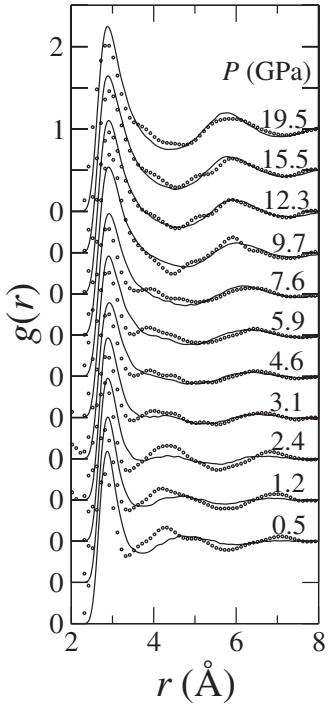

FIG. 4. Pressure dependence of the total pair distribution function $g(r)$ of liquid CdTe. The solid lines and open circles show the calculated and experimental (Ref. 6) results, respectively.

see that the plateau in $S(k)$ between $k=1.9$ and 2.8 Å^{-1} consists mainly of a broad peak of $S_{CdTe}(k)$. Above 4.6 GPa, a peak grows at $k=2.3$ Å^{-1} in $S_{CdCd}(k)$, and, in $S_{TeTe}(k)$, the peak at $k=1.9$ Å^{-1} becomes broad and the first minimum at $k=2.1$ Å^{-1} disappears. These changes in the like-ion correlations result in the appearance of the peak at $k=2.3$ Å^{-1} in $S(k)$ above 4.6 GPa. It is seen that the Te-Te correlation changes largely between 5.9 and 9.7 GPa, while $S_{CdCd}(k)$ and $S_{CdTe}(k)$ are almost unchanged. In $S_{TeTe}(k)$, the peak that exists at $k=1.9$ Å^{-1} below 5.9 GPa becomes weak with increasing pressure and almost disappears at 9.7 GPa. Instead, a peak appears at about $k=2.3$ Å^{-1} above 9.7 GPa. We see that the shift and sharpening of the first peak of $S(k)$ between 5.9 and 9.7 GPa come mainly from these changes in $S_{TeTe}(k)$. It is concluded from the observations in $S(k)$ and $S_{\alpha\beta}(k)$ that liquid CdTe at higher pressures ($P>8$ GPa) has a liquid form which is different from that at lower pressures ($P<4$ GPa), and there exists another liquid form at intermediate pressures ($4<P<8$ GPa). It is obvious that these structural changes are related mainly to the changes in the like-ion correlations.

B. Pair distribution functions

In Fig. 4, the total pair distribution function $g(r)$ is shown as a function of the pressure. The solid lines and open circles show the calculated and experimental[6] results, respectively. Although there are some discrepancies between them at lower pressures, the overall agreement on the pressure dependence is satisfactory. The pressure-induced changes observed in both the experimental and theoretical $g(r)$ are as follows. At 0.5 GPa, the first minimum and the second peak exist clearly, and the broad third peak can be seen around $r=7$ Å. With increasing pressure, the second peak shifts to smaller r, and the first minimum becomes shallower. Eventually, the minimum disappears, and the second peak becomes a shoulder of the first peak. At higher pressures ~19.5 GPa, there are no evidences of the first minimum and second peak that were observed at 0.5 GPa. The broad third peak around $r=7$ Å at 0.5 GPa also shifts to smaller r with increasing pressure. It grows with pressure and becomes a clear peak at about $r=5.8$ Å at 19.5 GPa.

The pressure dependence of the first-peak position r_1 and the coordination number N is shown in Fig. 5. The open and solid circles in Fig. 5(b) show the coordination numbers calculated as

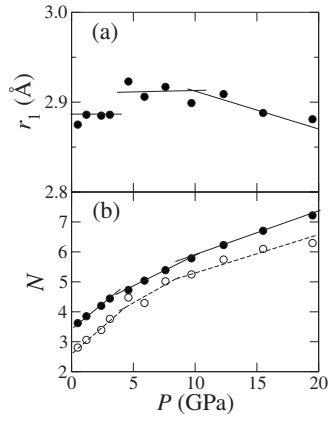

FIG. 5. (a) Pressure dependence of the first-peak position r_1 of $g(r)$. (b) Pressure dependence of the coordination numbers N calculated by two different definitions (see text).

$$N = 2\rho \int_0^{r_1} 4\pi r^2 g(r) dr \quad (1)$$

and

$$N = \rho \int_0^{R} 4\pi r^2 g(r) dr, \quad (2)$$

respectively, where ρ is the atomic number density. In the second definition, we used $R=3.4$ Å which was determined with reference to the first-minimum position at lower pressures. From Fig. 5, we see that the pressure changes of r_1 and N are not monotonic. Below 3.1 GPa, r_1 has weak pressure dependence. It increases abruptly at 4.6 GPa and decreases gradually above 10 GPa. Both N obtained by the two definitions increase with increasing pressure, and the increasing rate becomes low at higher pressures. The pressure variations of the two N are very similar to each other. Note that there are three pressure regions in the pressure dependence of r_1 and N corresponding to the three liquid forms observed in $S(k)$.

We should make some comments on the comparison with the experimental results. The coordination number N observed by the x-ray-diffraction measurements[6] shows abrupt increases at about 3 and 8 GPa with increasing pressure, while the calculated results do not show such sudden changes, as shown in Fig. 5(b). This difference would come from inadequacies of the approximations in the calculation method. We used two major approximations: the frozen-core approximation in the PAW method and the GGA in the DFT. We consider that the former is sufficient for our purposes because there are few mixed states related to the 4*d* states of Cd and 5*s* states of Te in the range of pressure we examined, as will be shown later. This indicates that the electrons in the electronic states of atoms, which have energies lower than the energies of those states, can be treated as the frozen cores. On the other hand, it is uncertain whether the latter approximation is sufficient or not, and the discrepancies between the experimental and theoretical results are likely to be caused by this approximation. However, we cannot discuss the quality of the calculations rigorously based only on the comparison of the coordination number because there are some ambiguities in the Fourier transform to obtain the real-space correlation from the experimental structure factor $S(k)$ with limited wave numbers. The direct comparison of $S(k)$ would be more reliable, as was shown in Fig. 1. Although not perfect, the agreement between the experimental and calculated results for the pressure dependence of $S(k)$ is rather good. Therefore, we believe that the qualitative features of pressure changes in partial quantities are correctly reproduced by our calculations.

The pressure dependence of the partial pair distribution functions $g_{\alpha\beta}(r)$ is displayed in Fig. 6. We see that, at 0.5 GPa, the first and second peaks of $g(r)$ consist mainly of the peaks of $g_{\mathrm{CdTe}}(r)$ and $g_{\mathrm{TeTe}}(r)$, respectively. It is clearly seen that the peak of $g_{\mathrm{TeTe}}(r)$ at about $r=4.7$ Å shifts to smaller r with increasing pressure, which results in the shift of the second peak of $g(r)$. At lower pressures ~0.5 GPa, the broad third peak of $g(r)$ at about 7 Å is mainly formed by

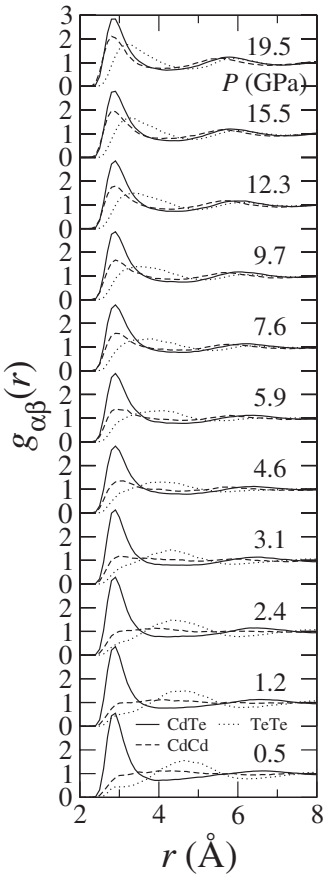

FIG. 6. Pressure dependence of the partial pair distribution functions $g_{\alpha\beta}(r)$ of liquid CdTe. The solid, dashed, and dotted lines show the correlations for $\alpha\beta$=CdTe, CdCd, and TeTe, respectively.

$g_{\mathrm{CdTe}}(r)$, and, at higher pressures ~19.5 GPa, the three correlations form the peak of $g(r)$ at about $r=5.8$ Å. Around $r=3$ Å, where the large first peak exists in $g_{\mathrm{CdTe}}(r)$, $g_{\mathrm{CdCd}}(r)$ and $g_{\mathrm{TeTe}}(r)$ have no clear peaks at 0.5 GPa, though they have finite values. The small shoulder at about $r=2.8$ Å in $g_{\mathrm{TeTe}}(r)$ would come from the covalent bonds between Te atoms as in the chain structure of pure liquid Te. Below 3.1 GPa, no remarkable changes in $g_{\mathrm{CdCd}}(r)$ and $g_{\mathrm{TeTe}}(r)$ are found. At 3.1–4.6 GPa, there appears a peak in $g_{\mathrm{CdCd}}(r)$, and it becomes higher with increasing pressure. At 7.6–9.7 GPa, $g_{\mathrm{TeTe}}(r)$ forms a broad peak around $r=3.5$ Å and becomes sharper at higher pressures. In this way, the correlations between like atoms around the first-coordination shell become more important with increasing pressure. To see this more clearly, we show the pressure dependence of the partial coordination numbers $N_{\alpha\beta}$ in Fig. 7. Since there are no clear first peaks in $g_{\mathrm{CdCd}}(r)$ and $g_{\mathrm{TeTe}}(r)$ at lower pressures, the second definition Eq. (2), is used to calculate N_{CdCd} and N_{TeTe}, which are shown in Figs. 7(a) and 7(b), respectively. N_{CdTe} is calculated by both the definitions and is displayed in Fig. 7(c). It is clearly seen from Fig. 7(a) that N_{CdCd} increases largely up to about 4 GPa, and its pressure dependence becomes weak above 4 GPa. On the other hand, we see that the increasing rate of N_{TeTe} changes around 8 GPa, as shown in Fig. 7(b). Both N_{CdCd} and N_{TeTe} increase by about 2 when the pressure is increased from 0 to 20 GPa, while N_{CdTe} in-

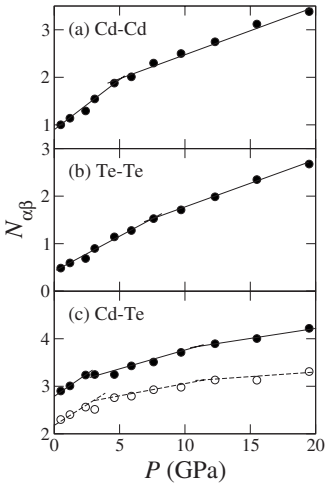

FIG. 7. Pressure dependence of the partial coordination numbers $N_{\alpha\beta}$ for $\alpha\beta$=(a) CdCd, (b) TeTe, and (c) CdTe, respectively.

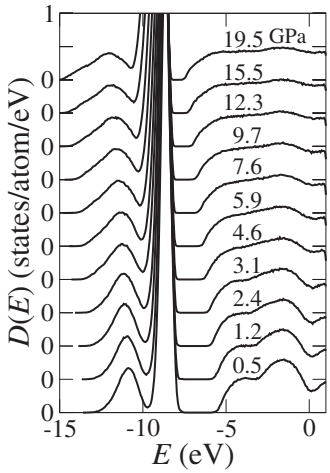

FIG. 8. Pressure dependence of the total electronic density of states $D(E)$ of liquid CdTe. The origin of energy is taken to be the Fermi level (E_F=0).

creases by only 1. These facts imply that the like-atom correlations are more important in the structural properties in liquid CdTe under pressure. We can say that the three forms observed in $S(k)$ are related to the appearance of the short-range correlations between like atoms. In the first form below 4 GPa, all three partial correlations have a weak pressure dependence, as shown in Fig. 6, and the coordination numbers increase, accompanying the volume reduction, as shown in Fig. 7. In the second form between 4 and 8 GPa, the Cd-Cd correlation becomes significant in the first-coordination shell as $g_{\mathrm{CdCd}}(r)$ has a clear peak at about r =3 Å. In the third form above 8 GPa, the Te-Te correlation at shorter distances becomes important, as $g_{\mathrm{TeTe}}(r)$ intrudes the first-coordination shell with a peak at about r =3.2–3.5 Å. Upon further compression, all the three partial correlations would become more similar to each other.

C. Electronic densities of states

Figure 8 shows the pressure dependence of the total electronic density of states (DOS) $D(E)$. Below 4 GPa, there is a dip at the Fermi level, which would correspond to the semiconducting properties of the liquid. The dip becomes shallower under further compression, and there is no structure at the Fermi level above 10 GPa. The energy range of the electronic states above E=−6 eV at 0.5 GPa spreads toward lower energies with increasing pressure. The position of the large peak at about E=−9 eV has almost no pressure dependence, while its width becomes wider at higher pressures. The peak around E=−11 eV shifts to lower energies, and its energy range spreads with compression.

The angular-momentum-dependent partial DOS $D^l_\alpha(E)$ is calculated from the weight of the angular momentum l for each electronic state,[19] which can be obtained from the population analysis described briefly in the next subsection. Figure 9 shows the pressure dependence of the partial DOS $D^l_\alpha(E)$. It is seen that, at 0.5 GPa, the electronic states above E=−6 eV consist of the 5s and 5p states of Cd and the 5p states of Te. As shown by the dashed lines in Fig. 9(b), $D^{5p}_{\mathrm{Te}}(E)$ has a large peak at about E=−1.5 eV and a shoulder around E=−4 eV, which correspond to mixed states with the 5p and 5s states of Cd, respectively. While these features are retained below 4 GPa, the peak of $D^{5p}_{\mathrm{Te}}(E)$ at about E=−1.5 eV becomes lower, and the peak height becomes comparable to the shoulder around E=−4 eV under further compression. The peaks of $D^{5s}_{\mathrm{Cd}}(E)$ and $D^{5p}_{\mathrm{Cd}}(E)$, shown by the thin solid and thin dashed lines in Fig. 9(a), respectively, become broader with increasing pressure. We see that $D^{5d}_{\mathrm{Te}}(E)$ increases above E=−5 eV with increasing pressure [the bold solid lines in Fig. 9(b)]. It is also seen that the electronic

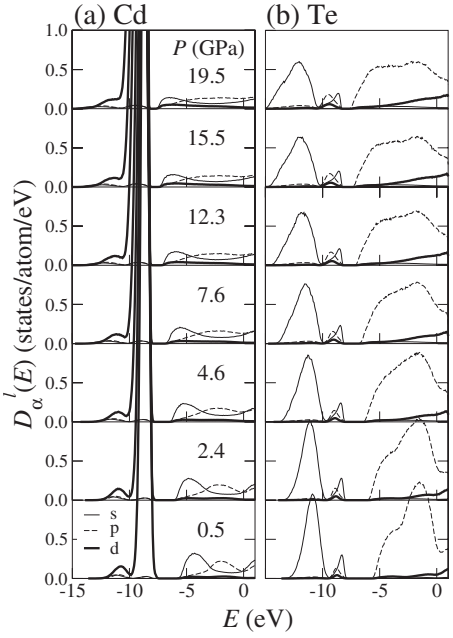

FIG. 9. Pressure dependence of the partial electronic densities of states $D^l_\alpha(E)$ of liquid CdTe for α=(a) Cd and (b) Te. The thin solid, thin dashed, and thick solid lines show $D^l_\alpha(E)$ for l=0, 1, and 2, respectively. The origin of energy is taken to be the Fermi level (E_F=0).

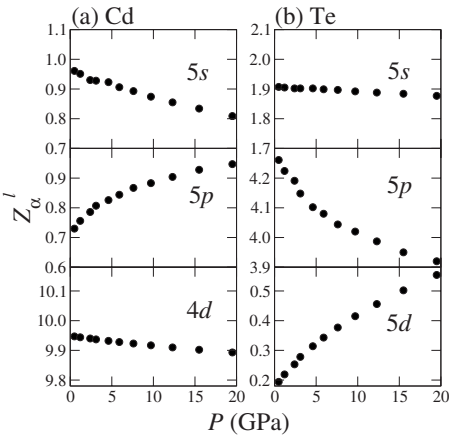

FIG. 10. Pressure dependence of the gross populations of electrons Z_α^l in the electronic state associated with the angular momentum l around α-type atoms.

states around $E=-9$ and -11 eV originate from the $4d$ states of Cd and the $5s$ states of Te, respectively.

D. Bonding properties

In this section, the bonding properties of liquid CdTe under pressure are discussed on the basis of the results of the population analysis.[20] By expanding the electronic wave functions in an atomic-orbital basis set,[19,21,22] we calculated the gross population of electrons Z_i^l in the electronic state associated with the angular momentum l around the ith atom and the bond-overlap population O_{ij} between the ith and jth atoms.[20] Since the atomic-orbital basis used in the expansion of the wave functions is not unique, a different set of atomic-orbital bases would give different values for Z_i^l and O_{ij}.[22] Therefore, we are unable to obtain the exact values of those quantities. However, their relative magnitudes can be discussed meaningfully because the trends are the same for any choice of atomic-orbital basis set. For the basis used in our calculations, the charge spillage[21] defining the error in the expansion is less than 0.2%.

Figure 10 shows the pressure dependence of the gross populations Z_α^l which were obtained by averaging $Z_{i\in\alpha}^l$ for α=Cd and Te. We see that Z_{Cd}^{4d} and Z_{Te}^{5s} depend weakly on pressure because these atomic electronic states are energetically isolated and do not form mixed states with other electronic states, as shown in Fig. 9. It is found that, with increasing pressure, Z_{Cd}^{5s} and Z_{Te}^{5p} decrease, and Z_{Cd}^{5p} and Z_{Te}^{5d} increase, which means that the electronic transitions of the $5s\rightarrow 5p$ and $5p\rightarrow 5d$ atomic electronic states occur around Cd and Te, respectively. Corresponding to the structural changes, the slope of the pressure variation of Z_α^l changes between 4 and 8 GPa except for the $4d$ states of Cd and the $5s$ states of Te.

Figure 11 shows the pressure dependence of the time-averaged distributions $p_{\alpha\beta}(\bar{O})$ of the overlap populations $O_{i\in\alpha,j\in\beta}$. Note that $p_{\alpha\beta}(\bar{O})$ is normalized so that the integration of $p_{\alpha\beta}(\bar{O})$, $\int_{O_{\min}}^{\infty} p_{\alpha\beta}(\bar{O})d\bar{O}$, gives the average number of β-type atoms that have overlap populations greater than $O_{\min}$

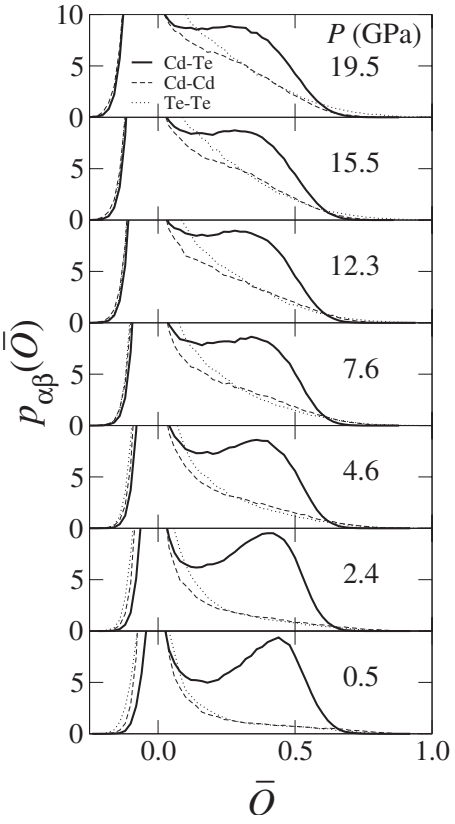

FIG. 11. Pressure dependence of the distributions $p_{\alpha\beta}(\bar{O})$ of bond-overlap populations $O_{i\in\alpha,j\in\beta}$. The solid, dashed, and dotted lines show $p_{\alpha\beta}(\bar{O})$ for $\alpha\beta$=CdTe, CdCd, and TeTe, respectively.

around one α-type atom. There are large peaks at $\bar{O}=0.0$ in the distributions of $p_{\alpha\beta}(\bar{O})$ because we calculated O_{ij} for pairs of atoms with a large cutoff distance ($\sim$8 Å). While finite values of O_{ij} are obtained for atomic pairs within the first-coordination shells, O_{ij} obtained for pairs with farther atomic distances are nearly zero and give the peaks at $\bar{O}=0.0$.

As shown by the solid lines in Fig. 11, below 4 GPa, $P_{\mathrm{CdTe}}(\bar{O})$ has a peak at about $\bar{O}=0.4$ with a clear minimum at about $\bar{O}=0.2$, while $P_{\mathrm{CdCd}}(\bar{O})$ and $P_{\mathrm{TeTe}}(\bar{O})$ have no peaks at finite $\bar{O}$. The existence of the peak in $P_{\mathrm{CdTe}}(\bar{O})$ indicates that there is a covalent-bonding interaction between Cd and Te atoms even in the liquid state, which is consistent with the presence of the gap in the DOS below 4 GPa (Fig. 8). At higher pressures above 4 GPa, the peak in $P_{\mathrm{CdTe}}(\bar{O})$ shifts to smaller $\bar{O}$, and the minimum becomes shallower, indicating that the covalent-bonding interaction weakens due to the metallization. Corresponding to the appearance of the correlations between like atoms in the first-coordination shell at higher pressures, $P_{\mathrm{CdCd}}(\bar{O})$ and $P_{\mathrm{TeTe}}(\bar{O})$ at larger $\bar{O}$ increase with increasing pressure.

E. Negative-slope melting curve

Here, we discuss the melting curve of CdTe under pressure based on our calculated results. It is known that the

melting temperature of CdTe decreases with increasing pressure up to about 2 GPa.[23] According to the Clausius–Clapeyron equation, the negative slope of the melting curve indicates that the liquid has a higher density compared to the solid.

The melting curve of group-IV elements, such as Si and Ge, also has a negative slope.[24] The crystalline phase of these elements has the fourfold coordinated diamond structure. Upon melting, the coordination number increases to about 6 with volume reduction. While the solid state has semiconducting properties, the liquid state is metallic. In this way, large differences exist in the structural and bonding properties between the solid and liquid states of group-IV elements. It is certain that the negative slope of the melting curve is closely related to these differences. In particular, the crucial origin of the negative-slope melting curve is considered to be the fact that the diamond structure has a sufficiently large open space that the liquid phase can be denser than the solid.[25]

It is seen from our calculations [Fig. 5(b)] as well as the x-ray-diffraction measurements[6] that the coordination number in liquid CdTe at pressures below 2 GPa is only about 4, which is similar to the value in the crystalline phase (zinc-blende structure). Also, we have seen that the covalent-bonding interaction between Cd and Te atoms is preserved in the liquid state below 4 GPa. From these observations, we conclude that, unlike liquid group-IV elements, the local properties of liquid CdTe at relatively lower pressures are similar to those of the solid state, which is consistent with the results of previous studies.[7,8] To consider the mechanism of the negative-slope melting curve of CdTe, we should notice that the octahedral space in the zinc-blende structure is sufficiently large as in the diamond structure. Since such large space is collapsed in the liquid state especially under pressure, the liquid is more closely packed than the solid, and the melting curve has a negative slope, even though each atom retains a nearly fourfold coordination.

Above 2 GPa, the crystalline phase transforms into a denser structure without such large space as the octahedral space in the zinc-blende structure, which gives the melting curve with a positive slope.[23]

IV. SUMMARY

The pressure dependence of the structural and electronic properties of liquid CdTe has been investigated by *ab initio* molecular dynamics simulations. The calculated structure factor $S(k)$ is in good agreement with the recent x-ray-diffraction measurements in a wide range of pressure. It has been confirmed that there are at least three forms in liquid CdTe under pressure up to 20 GPa, as observed experimentally. In the liquid form below 4 GPa, almost no short-range correlations exist between like atoms, and the liquid has semiconducting properties with the covalent-bonding interaction between Cd and Te atoms. Our simulations suggest that the high-pressure liquid forms are related to the appearance of like-atom correlations in the first-coordination shell, i.e., Cd-Cd and Te-Te correlations appear above 4 and 8 GPa, respectively, accompanying the metallization. The bonding properties have been examined by the population analysis, and it has been shown that the pressure dependence of Mulliken charges and bond-overlap populations correspond very well to that of the structure.

ACKNOWLEDGMENTS

The authors thank T. Hattori and K. Tsuji for providing us with their experimental data. The present work was supported in part by a Grant-in-Aid for Scientific Research on Priority Area, "Nanoionics (439)," and a Grant-in-Aid for Scientific Research (C) from MEXT, Japan. The authors thank the Supercomputer Center, Institute for Solid State Physics, University of Tokyo for the use of facilities.

[1] R. J. Nelmes, M. I. McMahon, N. G. Wright, and D. R. Allan, Phys. Rev. B **51**, 15723 (1995).
[2] T. Hattori, K. Tsuji, N. Taga, Y. Takasugi, and T. Mori, Phys. Rev. B **68**, 224106 (2003).
[3] T. Hattori, T. Kinoshita, T. Narushima, and K. Tsuji, J. Phys.: Condens. Matter **16**, S997 (2004).
[4] T. Hattori, T. Kinoshita, N. Taga, Y. Takasugi, T. Mori, and K. Tsuji, Phys. Rev. B **72**, 064205 (2005).
[5] T. Kinoshita, T. Hattori, T. Narushima, and K. Tsuji, Phys. Rev. B **72**, 060102(R) (2005).
[6] T. Hattori, T. Kinoshita, T. Narushima, K. Tsuji, and Y. Katayama, Phys. Rev. B **73**, 054203 (2006).
[7] V. V. Godlevsky, J. J. Derby, and J. R. Chelikowsky, Phys. Rev. Lett. **81**, 4959 (1998).
[8] V. V. Godlevsky, M. Jain, J. J. Derby, and J. R. Chelikowsky, Phys. Rev. B **60**, 8640 (1999).
[9] P. E. Blöchl, Phys. Rev. B **50**, 17953 (1994).
[10] G. Kresse and D. Joubert, Phys. Rev. B **59**, 1758 (1999).
[11] J. P. Perdew, K. Burke, and M. Ernzerhof, Phys. Rev. Lett. **77**, 3865 (1996).
[12] G. Kresse and J. Hafner, Phys. Rev. B **49**, 14251 (1994).
[13] F. Shimojo, R. K. Kalia, A. Nakano, and P. Vashishta, Comput. Phys. Commun. **140**, 303 (2001).
[14] S. Nosé, Mol. Phys. **52**, 255 (1984).
[15] W. G. Hoover, Phys. Rev. A **31**, 1695 (1985).
[16] M. Tuckerman, B. J. Berne and G. J. Martyna, J. Chem. Phys. **97**, 1990 (1992).
[17] O. H. Nielsen and R. M. Martin, Phys. Rev. B **32**, 3792 (1985).
[18] A. Dal Corso and R. Resta, Phys. Rev. B **50**, 4327 (1994).
[19] F. Shimojo, K. Hoshino and Y. Zempo, J. Phys. Soc. Jpn. **72**, 2822 (2003).
[20] R. S. Mulliken, J. Chem. Phys. **23**, 1833 (1955).
[21] D. Sánchez-Portal, E. Artacho, and J. M. Soler, J. Phys.: Condens. Matter **8**, 3859 (1996).
[22] M. D. Segall, R. Shah, C. J. Pickard, and M. C. Payne,

Phys. Rev. B **54**, 16317 (1996).
[23] A. Jayaraman, W. Klement, Jr., and G. C. Kennedy, Phys. Rev. **130**, 2277 (1963).
[24] S. N. Vaidya, J. Akella, and G. C. Kennedy, J. Phys. Chem. Solids **30**, 1411 (1969).
[25] G. L. Warren and W. E. Evenson, Phys. Rev. B **11**, 2979 (1975).